Distinct functional potential of bacterial extracellular vesicles across biogeographic provinces of the South Pacific Ocean

Eduard Fadeev[1,*], Neza Orel[2], Tinkara Tinta[2], Leila Afjehi-Sadat[3], Haoran Liu[4], Thomas J. Browning[4], Zhongwei Yuan[4], Eric P. Achterberg[4], Steven J. Biller[5], Daniel J. Sher[6], and Gerhard J. Herndl[1,3,7]

[1] Department of Functional and Evolutionary Ecology, Bio-Oceanography and Marine Biology Unit, University of Vienna, Vienna, Austria

[2] Marine Biology Station Piran, National Institute of Biology, Piran, Slovenia

[3] Mass Spectrometry Unit, Research Support Facilities, University of Vienna, Vienna, Austria

[4] GEOMAR Helmholtz Centre for Ocean Research, Kiel, Germany

[5] Department of Biological Sciences, Wellesley College, Wellesley, USA

[6] Department of Marine Biology, Leon H. Charney School of Marine Sciences, University of Haifa, Haifa, Israel

[7] NIOZ, Department of Marine Microbiology and Biogeochemistry, Royal Netherlands Institute for Sea Research, Den Burg, The Netherlands

*Corresponding author

Keywords: bacterioplankton, membrane vesicles, horizontal gene transfer, siderophores, extracellular enzymes

Abstract

Bacterial extracellular vesicles (BEVs) are spherical membrane-bound structures released by bacterial cells that can carry various biological compounds. Experimental investigation of BEVs in marine bacteria, largely limited to laboratory model systems, have suggested putative roles in bacterial ecophysiology. Yet the functions of BEVs in their ecological context has never been explored directly in the ocean. Here we report the results a large-scale oceanographic survey of marine BEVs in surface waters, conducted over more than 5,000 nautical miles in the South Pacific, linking their protein cargoes to the bacterial communities producing them. The presence of marine BEVs was consistently observed across a range of biogeochemical conditions, with an overall abundance comparable to that of bacterial cells (ca. 10^8 BEVs L^{-1}). The protein cargoes of marine BEVs differed significantly between environmental conditions, being enriched in carbohydrate transporters and hydrolytic enzymes under phytoplankton bloom conditions, and enriched in iron uptake-related proteins in nutrient-limited waters, suggesting key extracellular functions they could perform in marine bacterial communities. Our observations highlight the ubiquity of marine BEVs and their potential functions across oceanic scales, with implications for our general understanding of key processes in marine microbial ecology.

Introduction

Bacterial extracellular vesicles (BEVs) are spherical membranous structures typically ranging between 20 and 250 nm in diameter that can carry various biological cargoes (e.g., nucleic acids and proteins) over long distances in a protected and locally concentrated manner [1]. Since their discovery in human-associated *Escherichia coli* in the 1960s [2], most research on BEVs has focused on pathogens and other host-associated bacteria [3]. Although it remains unclear to what extent the release of BEVs is an active cellular process or simply a by-product of cell growth or death (i.e., lysis), a variety of BEV functions have been described to date. One of the best-documented functions of BEVs is the intercellular transfer of DNA molecules [4,5], which can facilitate the exchange of antibiotic resistance genes between different bacterial lineages [6], as well as the transfer of entire plasmids [7,8], recently termed 'vesiduction' [9]. In addition to DNA transfer, BEVs can also play a role in bacterial quorum sensing [10,11], biofilm formation [12], and contribute to microbial "warfare", where they deliver compounds that kill competing bacteria [13,14].

Because BEVs contain fragments of the releasing bacterial cell, as well as cell membrane-derived enzymes, receptors and transporters, it has been proposed that BEVs may have a variety of functions in the exocellular milieu [15,16] in addition to intercellular interactions, which may be particularly relevant for bacteria living in aqueous environments [3,17]. The ocean - the largest aquatic ecosystem on Earth where bacteria are among the most abundant organisms [18] - is a highly dynamic environment both physically and biochemically. The surface waters of the ocean are characterised by a depletion of bioavailable nutrients required for life in some areas (e.g., oceanic gyres) [19] and a high availability in others (e.g., coastal upwelling regions) [20,21]. To survive in such dynamic ecosystems, marine bacteria have developed a wide range of ecophysiological capabilities [22–24], and implement highly diverse nutrient and energy utilisation strategies [25–27]. In the interaction between marine bacteria and their nutrient depleted environment, high cellular surface area to volume ratios provide optimal conditions for nutrient uptake [28,29]. In this sense, marine BEVs can be conceptualised as an expansion of the cell surface [1] that diffuses through seawater and randomly encounters biotic and abiotic components. Existing laboratory-based observations of several isolates of globally abundant marine bacteria [30–35] suggest that BEVs may mediate specific extracellular functions in the ecophysiology of marine bacteria, such as binding specific elements (e.g., iron or phosphate) and delivering them in concentrated form to bacterial cells. However, despite the apparent ubiquity of BEVs in the marine environment [36,37] and their potential ability to impact bacterial functions, how the contents and functional potential of these nanoparticles might vary across broad oceanographic contexts is unknown.

In this study we determined the abundance and protein cargo diversity of BEVs across the surface waters of the South Pacific Ocean. By combining molecular characterisation of marine BEVs with their local microbial and biogeochemical context, we show that BEV contents vary among ocean regions and may contribute to acquisition of limiting nutrients by the local microbial community. Our observations across a large oceanic basin reinforce the hypothesis that important extracellular bacterial functions may be mediated by BEVs in the global ocean.

Results and Discussion

Distinct biogeochemical conditions across the South Pacific Ocean

To investigate the potential ecophysiological functions of BEVs in marine bacterial communities we sampled across diverse environmental conditions, varying in nutrient limitations and phytoplankton bloom conditions. We collected surface water (5-6 m depth) at 20 stations along a transect that spanned the South Pacific Ocean (Fig. 1A; Table S1). Detailed physicochemical characterization across this transect [38], showed that the field sampling was carried out across four oceanic provinces. Briefly, the easternmost region was the Chilean coastal upwelling zone (UP), characterised by elevated nitrate and phosphate concentrations, while depleted in dissolved iron. In this area there were elevated chlorophyll-a concentrations (ca. 3 mg m^{-3}; Fig. S1), with the phytoplankton community mostly composed of diatoms (Fig. 1B). The transition zone between the upwelling and the subtropical gyre (TRAN) was

characterised by elevated concentrations of phosphate and dissolved iron, but depleted in nitrate. This area also had relatively high chlorophyll-a concentrations (0.04-0.26 mg m^{-3}), with mixed phytoplankton communities. The centre of the subtropical gyre (GYRE) was characterised by very low nitrate concentrations and a declining spatial gradient from east to west of phosphate concentrations, with very low chlorophyll-a concentrations (< 0.03 mg m^{-3}). The westernmost region (WEST) was defined as the area of the subtropical gyre with the lowest phosphate concentrations (< 10 nM) and higher (compared to GYRE) chlorophyll-a concentrations (0.03-0.14 mg m^{-3}) of predominantly cyanobacterial origins.

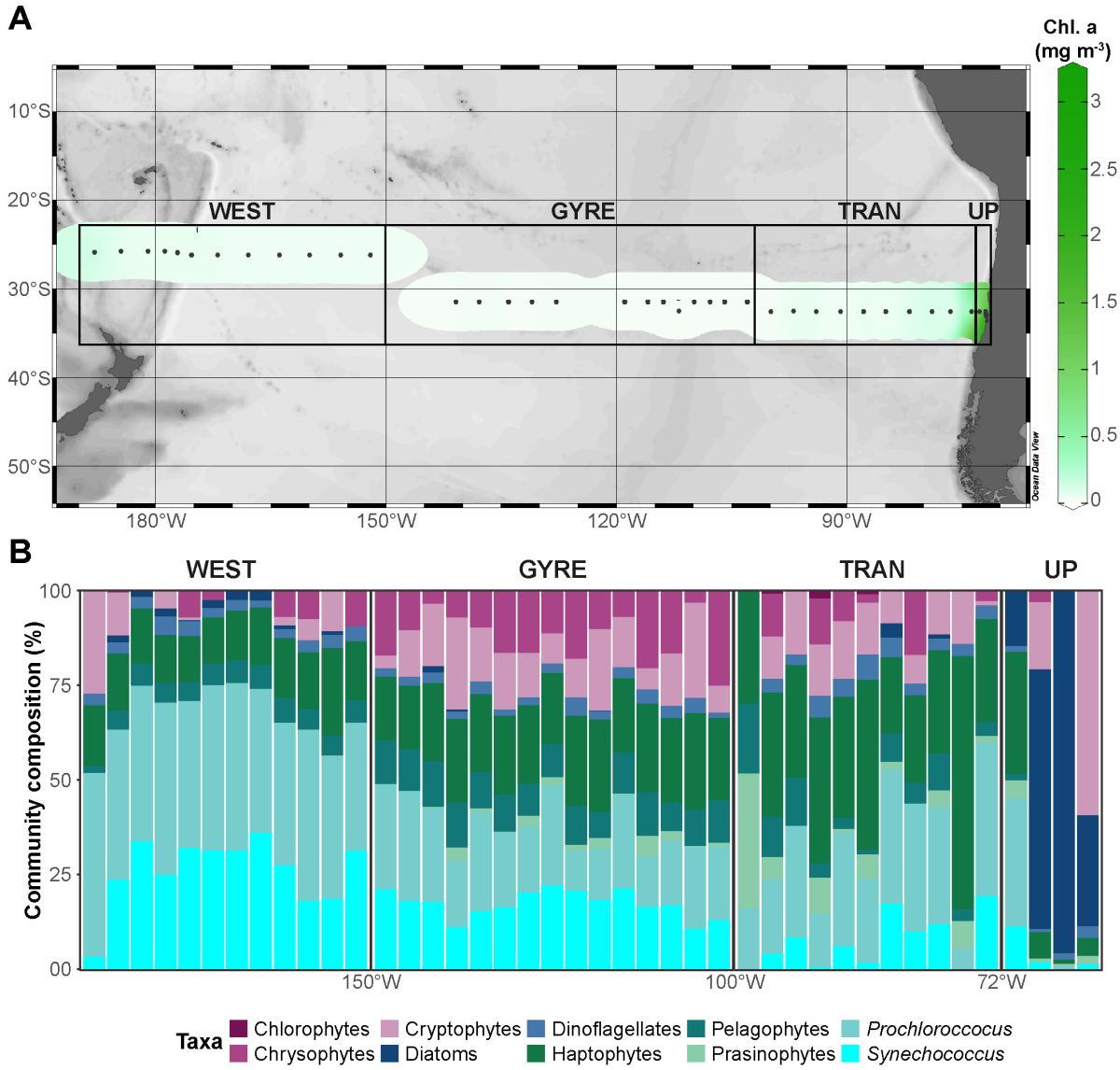

Fig. 1 – Diverse biogeochemical regimes encountered across the South Pacific Ocean. *(A) Spatial grouping of the sampling stations according to the four oceanic provinces: 'UP' - Chilean coastal upwelling zone; 'TRAN' - transition zone between the upwelling and the subtropical gyre; 'GYRE' - South Pacific subtropical gyre; 'WEST' - westernmost region. Chl. a concentration is overlaid on the cruise transect, with the grey scale background representing the bathymetry.(B) The composition of the surface water phytoplankton at each station, estimated on the basis of diagnostic pigments.*

We found that bacterial abundance (analysed using flow cytometry) varied between the biogeochemical provinces, and the taxonomic composition of the bacterial communities (based on metagenomic characterisation) also differed significantly between them (Fig. 2; PERMANOVA test; $F_{3,14}$=21.16, R^2=0.82, p=0.001). To investigate the physiological and metabolic processes expressed within the bacterial communities, we characterised the proteome of the bacterial cells, identifying between 4504-

6532 cellular proteins at each station (Table S1). The composition of bacterial cellular proteins was significantly different between the four regions (Fig. S2; PERMANOVA test; $F_{3,16}$=2.85, R^2=0.35, p=0.001). To test for the differences between the physiological and metabolic processes in bacterial communities in the different provinces, we performed differential protein abundance analyses between each pair of adjacent provinces (Table S2). The bacterial abundance was strongly elevated in the upwelling zone (9-26×10^8 cells L^{-1}), with the bacterial community showing a strong heterotrophic response to the availability of organic carbon as a result of the diatom bloom. The dominant bacteria were *Flavobacteriales* and *Cellvibrionales*, which are typically active during phytoplankton blooms [39,40]. In the transition zone, bacterial abundance reached 0.4-3.5×10^8 cells L^{-1}, with an elevated photosynthetic activity of the cyanobacterial order *Synechococcales* (*Prochlorococcaceae* and *Synechococcaceae*), which was probably stimulated by a nutrient influx from a returning lateral current [38]. The subtropical gyre exhibited the lowest bacterial abundances (0.2-0.9×10^8 cells L^{-1}), characterised by the dominance of the oligotrophic order *Pelagibacterales* [41], which has previously been shown to numerically dominate the bacterial communities of the ultra-oligotrophic South Pacific subtropical gyre [42,43]. In the westernmost region, bacterial abundance was significantly higher than in the subtropical gyre (0.8-1.3×10^8 cells L^{-1}; Student's t-test, p=0.002), characterised by increased activity of *Prochlorococcaceae*, which may have been partly facilitated by micronutrient input from a large volcanic eruption in the region two months prior to sampling [44].

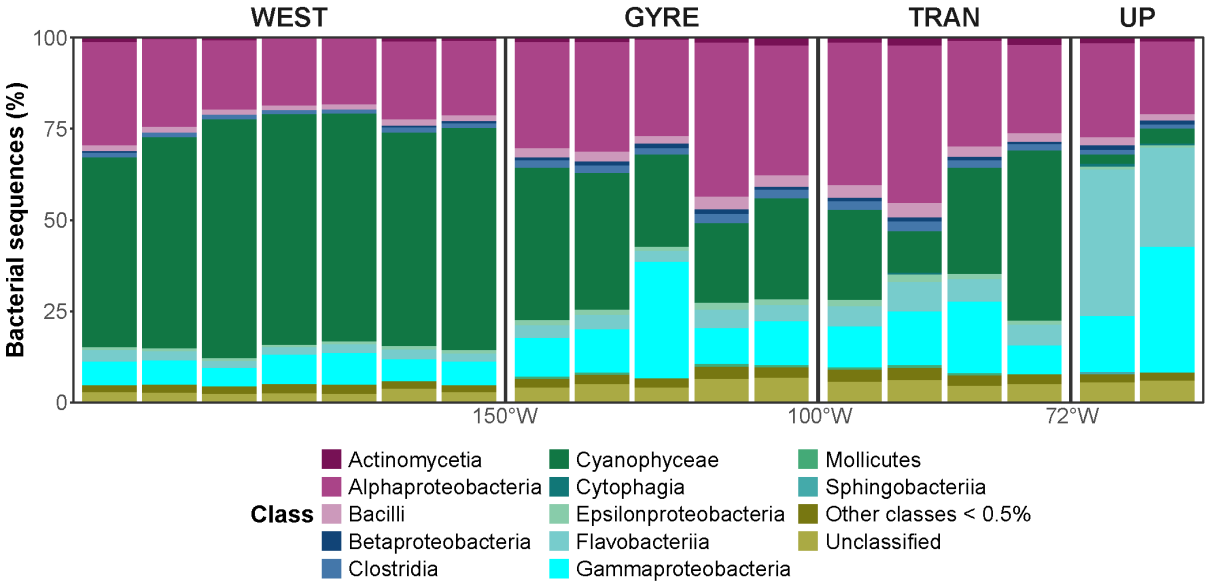

Fig. 2 – Bacterial community composition based on taxonomic classification of metagenomic sequences. *'Other classes < 0.5%' – refers to taxonomic classes that comprised less than 0.5% of the sequences; 'unclassified' – refers to bacterial sequences with unknown classification on a class level. All samples contained 2-5×10^8 classified sequences.*

Abundance and characteristics of marine BEVs

To investigate the abundance and diversity of marine BEVs, we sampled the extracellular size fraction corresponding to BEV-like structures (100 kDa-0.22 µm) across all stations using size fractionated filtration. To some extent, marine viruses are in the same size fraction as BEVs, and they can be a major obstacle to studying marine BEVs due to our limited ability to mechanically separate them [45–47]. Therefore, we used density gradient separation to further enrich each sample for BEVs in the laboratory (see Materials and Methods). At least 50% of the purified BEVs were in the 70 to 130 nm diameter range, matching the size distributions reported for cultures of marine bacteria (Fig. S3)[33,35]. The abundance of BEVs was in the same order of magnitude as bacterial cells (Fig. 3). However, because the density gradient separation resulted in a reduced yield of 6-52% of all nanoparticles (Fig. S4), these are likely conservative estimates of the BEVs concentration in the seawater. We then characterised the

protein cargoes of the BEV-like structures and identified 2029-3580 BEV-associated proteins at each station (Table S1). Of these proteins only 56-121 were taxonomically or functionally (e.g., capsid or tail sheath) related to viruses, suggesting a strong enrichment of BEVs in our samples. We found that 78-96% of proteins observed in the BEVs were also found in the corresponding cellular fraction at each station, but the composition of the proteins significantly varied between the two fractions (PERMANOVA test; $F_{1,38}$=15.00, R^2=0.28, p =0.001). This indicates that the BEVs represent a subset that differs from the full bacterial proteome.

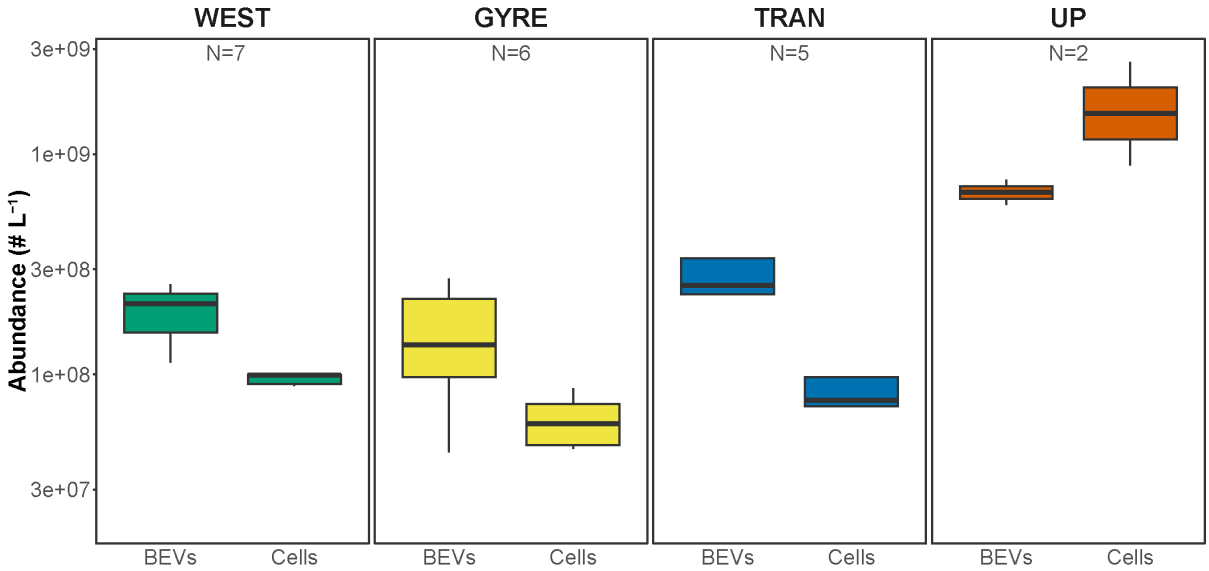

Fig. 3 – Bacterial cell and EVs abundances across different provinces. *The abundances were determined by flow cytometry and nanoparticle tracking analysis (NTA), respectively. The N represents the number of stations in each province.*

Gram-negative marine bacteria can release BEVs through blebbing of the cellular membrane, forming particles bounded by fragments of cellular membranes and containing periplasm of the releasing bacterial cell [1,48]. In addition to biases in packaging relating to subcellular localization, external factors have also been shown to have an impact on the production of BEVs and their contents [49–52]. Other BEVs may result from bacterial cell lysis due to bacteriophages, and thus represent a pseudo-random assemblage of fragments from different subcellular origins [3,53]. To differentiate between these different origins of BEVs, we assessed whether there is an enrichment in non-cytoplasmic proteins in the BEV fraction. Overall, we identified 1,121 proteins that were significantly enriched in BEVs compared to the cellular fraction across the dataset ($\log_2$ fold change >1, adjusted p-value < 0.1; Table S3). Prediction of sub-cellular origins revealed that half of the BEV-enriched proteins were non-cytoplasmic, comprising mostly outer membrane and extracellular proteins, compared to ca. 25% of the enriched proteins in the cellular fraction (Fig. 4). Although we cannot specifically identify their production process in our dataset, our results suggest that the packaging of marine BEVs is strongly biased towards proteins of non-cytoplasmic origin.

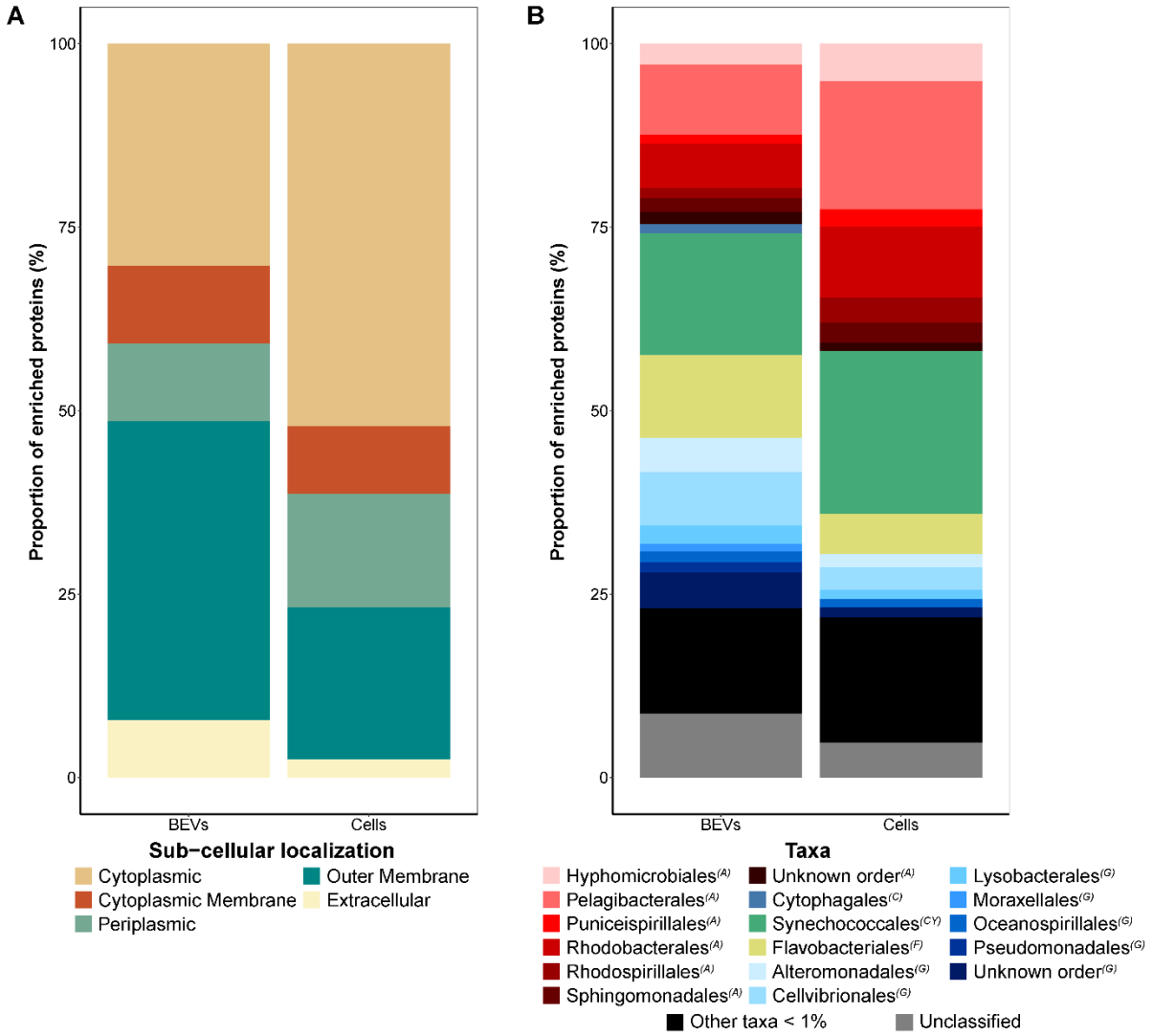

Fig. 4 – Proportions of significantly enriched proteins between BEV and cellular fractions. *Proportion of enriched proteins in each fraction according to their predicted sub-cellular origins (A) and taxonomic affiliation (B). The total number of enriched proteins in the BEVs and the cellular fractions was 1121 and 2075, respectively. Taxonomic affiliations of enriched proteins in the cellular and BEVs fractions according to different oceanic provinces. The taxonomic class of each order is given in parentheses: 'A' – Alphaproteobacterial, 'C' – Cytophagia, 'CY' – Cyanophyceae, 'F' – Flavobacteriia, 'G' – Gammaproteobacteria.*

The enrichment analyses revealed that proteins associated with the cyanobacterial order *Synechococcales* (families *Prochlorococcaceae* and *Synechococcaceae*) made up the largest number of enriched proteins in the BEVs and cellular fractions, proportionally accounting for 17% and 22% of proteins, respectively (Fig. 4). The second largest taxonomic group was the order *Pelagibacterales* (the SAR11 clade of Alphaproteobacteria), which accounted for 9% of BEV-enriched proteins while comprising 18% of enriched proteins in the cellular fraction. In contrast, enriched proteins associated with other bacterial orders, such as *Flavobacteriales* (mostly the family *Flavobacteriaceae*), *Alteromonadales* (mostly the families *Alteromonadaceae* and *Pseudoalteromonadaceae*), and *Cellvibrionales* (mostly the families *Halieaceae* and *Cellvibrionaceae*), accounted for more than twice the relative amount of BEV-enriched proteins compared to the cellular fraction. A previous comparison of isolates from the major classes of marine bacteria suggested that there may be a relationship between growth and BEVs production rates [35]. Based on the assumption that the number of enriched proteins

184 reflects the abundance of BEVs to some extent, our results support the previously raised hypothesis that
185 fast-growing bacteria (e.g. *Flavobacteria* and *Alteromonas*) contribute more to the BEVs population [35].

186 It has been postulated that the production of BEVs is influenced by environmental factors that affect
187 their potential ecological impact [16,35]. Therefore, to account for the differences in microbial communities
188 and the biogeochemical conditions, we further examined each oceanic province separately. To infer the
189 potential functions of BEVs in the interaction with the extracellular environment, we examined 2,700
190 outer membrane and extracellular proteins identified in our dataset for enrichment in BEVs. We found
191 a total of 608 of these proteins (Table S4), which were associated with 51 different bacterial lineages
192 (Fig. S5), that were significantly enriched in BEVs compared to bacterial cells. The BEV-enriched
193 proteins were found to be associated with a variety of functional groups, including solute-binding
194 proteins, porins and various ribosomal proteins, as well as numerous proteins whose function is
195 unknown. Different proteins were found enriched in BEVs in different oceanic provinces, suggesting
196 that BEVs may play a role in multiple ecophysiological processes, the main ones of which are discussed
197 below.

198 **Marine BEVs as vectors for iron scavenging**

199 Iron is a micronutrient that occurs at low concentrations in surface seawater but is vital for life [54]. Iron
200 limitation can lead to enhanced BEVs production in non-marine bacteria [55]. Preferential packaging of
201 iron-related transporters into BEVs has been proposed to facilitate iron accumulation [52,56,57], and
202 subsequent uptake of such BEVs by bacterial cells has previously been demonstrated in a culture of a
203 pathogenic Gammaproteobacteria [58]. To scavenge for iron in the environment, some marine bacteria
204 release siderophores that strongly bind iron, and are subsequently acquired by bacterial cells through
205 specialised TonB-dependent transport systems [59–61]. The largest group of proteins that were significantly
206 enriched in marine BEVs consisted of proteins related to the TonB-dependent transport system (Fig. 5),
207 which accounted for 34-47% of all BEV-enriched outer membrane proteins in each region, compared
208 to 22-27% of outer membrane proteins enriched in the cellular fraction (Table S3). The majority of
209 these proteins were TonB-dependent receptors, which are outer membrane proteins that perform high-
210 affinity binding and energy-dependent transport of specific substrates across the membrane [62]. Although
211 the exact substrate for most of these receptors is unknown, we were able to identify 7 siderophore-
212 specific TonB-dependent receptors that were enriched in the BEVs across the transect. To actively
213 transport the siderophore across the outer membrane, the TonB-dependent receptor requires proton
214 motive force from the inner membrane [62]. While a proton motive force is likely lacking in BEVs, it has
215 recently been demonstrated in a non-marine bacterial isolate that TonB-dependent receptors are capable
216 of binding the siderophores even in the absence of such an energy source [58]. Therefore, it is possible
217 that iron or iron-rich proteins are trapped on the BEVs even if they are not internalized.

218 While production of siderophores in marine bacterial communities is mostly restricted to the class
219 Gammaproteobacteria, the capacity to acquire them from the environment (i.e., synthesizing specific
220 TonB-dependent receptors) is a taxonomically widespread functional trait [22]. Nonetheless, the vast
221 majority of the BEV-enriched TonB-dependent receptors we observed was also assigned to members
222 of the class Gammaproteobacteria (orders *Alteromonadales* and *Cellvibrionales*, as well as other
223 unclassified lineages), which represented 20-28% of all BEV-enriched outer membrane proteins,
224 compared to 12-16% of outer membrane proteins enriched in the cellular fraction. Enrichment of TonB-
225 dependent receptors on BEVs has been previously observed in cultures of marine Gammaproteobacteria
226 [31,63], among which are also several isolates of the order *Alteromonadales* [32]. Members of
227 *Alteromonadales* are copiotrophs that thrive under high availability of organic matter [64] and are
228 considered to be major siderophore producers and key mediators of iron acquisition in marine bacterial
229 communities [65,66]. We propose that during episodes of high metabolic activity (e.g., associated with
230 increased primary production), *Alteromonadales* not only release siderophores that bind dissolved iron,
231 but also produce BEVs that 'concentrate' them in the environment.

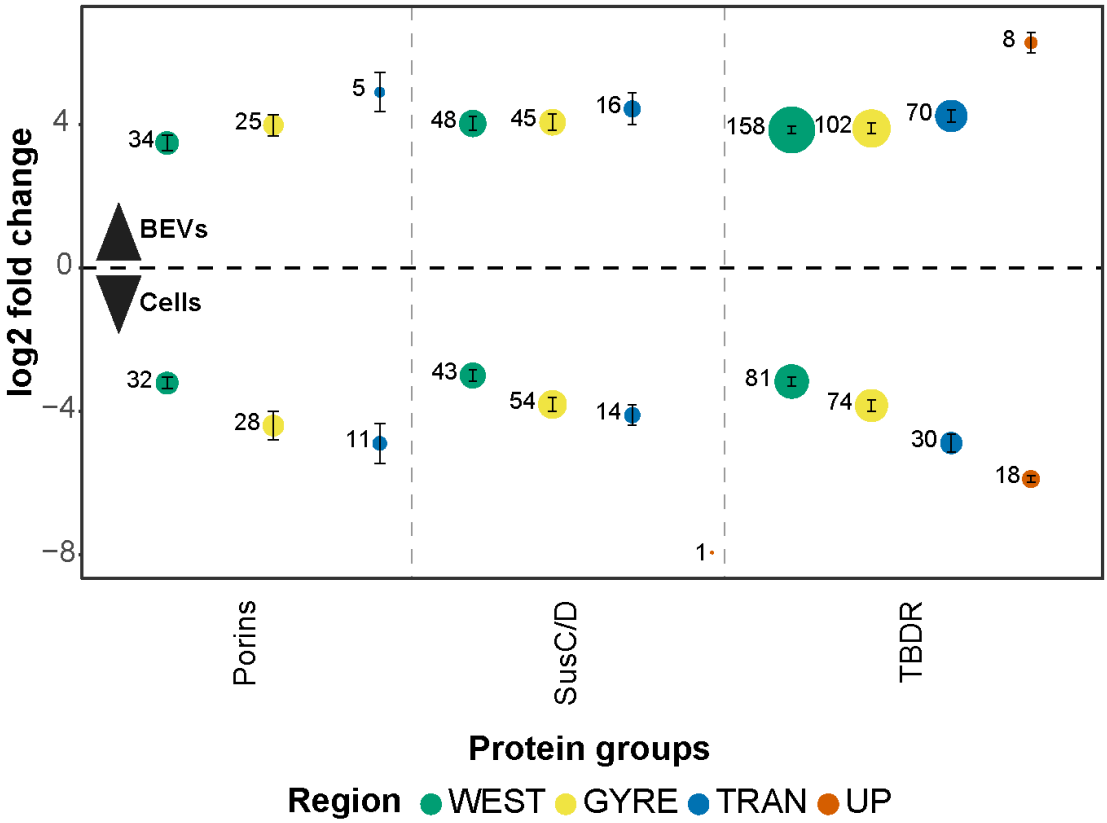

Fig. 5 – Enrichment of selected groups of proteins in marine BEVs. *The upper panel shows the enrichment in BEVs and the lower panel shows the enrichment in the cellular fraction. 'Porins' – includes the cyanobacterial iron-specific porins and the putative carbohydrate-selective porin OprB.'SusC/D' - includes both the SusC- and SusD-like proteins of the flavobacterial carbohydrate transport system. 'TBDR' – includes various TonB-dependent receptors. The total number of enriched proteins is indicated by the size of each circle and the number next to it.*

Along with nitrogen, iron was the limiting nutrient of surface water primary production across most of the oceanic transect [38]. In the transition zone, where there was an elevated cyanobacterial activity without iron limitation, we did not identify any iron-selective porins among the BEV-enriched cyanobacterial proteins, compared to 6 enriched porins in the cellular fraction (Table S4). In contrast, in the westernmost region, where a cyanobacterial activity was observed and iron was identified as one of the limiting nutrients, 14 of the 37 BEV-enriched proteins associated with cyanobacteria (mostly *Prochlorococcaceae*) were putative iron-selective porins (Fig. 5). We propose that these iron-specific porins form channels that allow passive diffusion of inorganic iron into the BEVs, as they would do in intact cells [67]. The inorganic iron could then be bound by periplasmic iron-binding proteins [68], trapping it inside the BEVs.

In ocean regions with limited iron availability, BEVs with the characteristics described above could be considered as nanoscale "hotspots" of bioavailable iron that could potentially be available to marine bacteria in a relatively concentrated form. The producers of these BEVs could be either pelagic (i.e., free-living)[34,35], particle-associated [32,63], or associated with phytoplankton cells [30]. The BEVs produced by particle- or phytoplankton-associated bacteria are (to some extent) likely to be taken up by the same type of cell, since particle-associated bacteria may live in "microcolonies" [69,70]. By contrast, the cells found in the vicinity of a pelagic bacterium are likely to be distinct from the bacterium itself [71]. Although we still lack a thorough understanding of iron-related interactions among pelagic marine bacteria [72], we propose two possible mechanisms for the role of BEVs in iron acquisition by marine bacterial communities. One possible scenario is that, similar to siderophores that can be taken up by different

259 taxa [22], and these iron-accumulating marine BEVs could be considered to some extent as 'public goods'
260 that facilitate the iron needs of the entire bacterial community. However, it has also been shown that in
261 some cases the uptake of BEVs can be selective towards closely related bacterial lineages [56]. Although
262 the direct recognition mechanism between bacterial cells and BEVs [73], and the indirect effect of
263 characteristics such as lipid composition and surface charge on BEV uptake remain poorly understood,
264 the available evidence suggests that biases may exist within cell-vesicle interactions. Therefore, the
265 release of iron-accumulating BEVs could also be a means of competing for iron in the marine
266 environment, potentially favouring only closely related phylogenetic populations.

267 **Marine BEVs as mediators of extracellular carbohydrate turnover**

268 Some "selfish" marine bacteria have developed a strategy to prevent the loss of BEVs through
269 dispersion by producing them in chains that remain partially attached to the cell [30,31]. Such chains were
270 first observed in an isolate of *Formosa* spp. (class Flavobacteriia), and also in an isolate of marine
271 *Pseudoalteromonas* (class Gammaproteobacteria), where they were proposed to play a role in
272 carbohydrate utilisation based on the transporters and hydrolytic enzyme content of the BEVs.
273 Flavobacteria are predominantly active during elevated availability of organic matter (e.g., during
274 phytoplankton blooms), efficiently utilising various carbohydrates using their unique SusC/D transport
275 system [74,75]. Such BEV chains are fragile and were likely detached and disrupted by our filtration steps
276 [30], ending up in the bulk BEVs fraction. In our dataset, we identified 57 different integral SusC-like
277 TonB-dependent transporters that were enriched in the BEVs and 79 SusC-like proteins enriched in the
278 cellular fraction, with an absolute $\log_2$ fold change of around 4 (Fig. 5). In contrast, the 25 different
279 extracellular glycan-binding SusD-like proteins, which sit on top of the SusC and bind the substrate [76],
280 comprised more than twice the number of proteins in the BEV fraction than in the cellular fraction, with
281 an absolute $\log_2$ fold change of 4-5 compared to 2-4. Taken together with other BEV-enriched
282 flavobacterial proteins (Table S3), our observations are highly consistent with the previously conducted
283 culture-based study of *Formosa* spp. [30], confirming that flavobacterial BEVs with similar protein
284 content also occur in the natural marine environment.

285 The SusC/D transport system requires energy from the inner membrane in order to transport substrate
286 across the outer membrane [76]. In *Formosa* spp., based on protein characterization, it has been suggested
287 that the BEV-chains contain to some extent also an inner membrane (indications for which we also
288 observed here, such as the inner membrane SecDF protein and the ExbB proton pump; Table S3), and
289 so it is conceivable that BEV chains may have some ability to take up carbohydrate molecules, which
290 are then transported into the cell [30]. However, the stronger enrichment of SusD-like lipoproteins in the
291 BEV fraction compared with SusC suggests a similar mechanism to that proposed above for TonB-
292 dependent receptors, in which such flavobacterial BEVs are more likely to only be able to bind
293 carbohydrate molecules. The trapping of carbohydrate molecules on the cell membrane has been shown
294 to facilitate their efficient digestion by hydrolytic enzymes [26]. Recent observations have shown that gut
295 bacteria can actively alter the enzyme content of BEVs to optimise carbohydrate utilisation [77], an
296 analogous process may occur also in marine bacteria. While we lack such a mechanistic understanding
297 for marine BEVs, the presence of hydrolytic enzymes associated with BEVs and their activity has been
298 observed in several isolates of heterotrophic marine bacteria [31,32,78,79]. We were also able to identify a
299 single carbohydrate active enzyme (CAZyme - glycoside hydrolase family 16), taxonomically assigned
300 to *Flavobacteriales* that was enriched in BEVs in the westernmost region (Table S4). We also identified
301 an additional glycoside hydrolase taxonomically affiliated with the Alteromonadales and significantly
302 enriched in BEVs across the entire transect. Conceptually, the association of enzymes with marine
303 BEVs is advantageous because it allows them to be delivered to the substrate in a more protected manner
304 compared to direct excretion, and may also allow for more efficient degradation due to the higher
305 concentration of enzymes that ultimately reach the target molecule [1]. While it is widely accepted that
306 marine bacteria release hydrolytic enzymes into the extracellular milieu to facilitate carbohydrate
307 degradation [80], the evidence above suggests that part of this secretion occurs via marine BEVs.

Conclusions

Here we have characterised the abundance and diversity of marine BEVs on an extensive oceanic scale, integrating their ecological and biogeochemical contexts. We found that marine BEVs are ubiquitous in seawater and possess a substantial degree of protein diversity. A relationship was identified between the enrichment of certain cargoes of BEVs and the ecological conditions experienced by the local bacterial community, thus confirming their potential role in the scavenging of extracellular nutrients and energy. The next stage of the research requires methodological investigation into the mechanisms underlying BEV uptake, as this is a major gap in our understanding of the relationship between BEVs and bacterial cells. It also requires quantitative experiments on the contribution of BEVs to extracellular enzymatic activity and iron accumulation in marine bacterial communities. We argue that future research on extracellular processes in marine bacterial communities should consider the possibility that characterisations of bulk seawater may conflate activity mediated by 'truly' dissolved molecules (e.g. siderophores and enzymes) with activity associated with BEVs, the products of which may not be equally available to all cells.

Materials and Methods

Sample collection

The oceanographic sampling was conducted onboard RV *Sonne* (cruise SO289 representing section GP21 of the GEOTRACES program) from 18 February to 8 April 2022 (Fig. 1). Water samples with a total volume of 60 L were taken from a depth of ca. 6 m at each sampling station using the onboard water pump. To remove particulate matter and eukaryotic cells, water samples were pre-filtered at low pressure using a 3 µm pore-size membrane filter (Merck Millipore, MA, USA). From the pre-filtered water sample, 1 mL was preserved with 4% glutaraldehyde (final concentration) and stored at -80°C until flow cytometric analysis. The pre-filtered seawater sample was then filtered through a 142 mm diameter polycarbonate filter with a pore-size of 0.22 µm (Merck Millipore, MA, USA), which was then stored at -80°C and later used for molecular analyses of the bacterial communities. The filtrate (< 0.22 µm) was concentrated ca. 60 times using a Vivaflow tangential flow filtration system (Sartorius, Germany) with a 100 kDa cut-off to 1 L and stored at -20°C until further BEVs purification in the laboratory.

Phytoplankton pigments analysis

Seawater samples (2-4 L) for diagnostic phytoplankton pigments were filtered onto MF300 glass fibre filters (ThermoFisher Scientific, MA, USA) and stored at -80°C until analysis. Pigment extraction and analysis followed the procedure described by [19]. Briefly, upon return to a land-based laboratory, pigments were extracted in 90% acetone by homogenization of the filters using glass beads in a cell mill, centrifuged (10 minutes, 5200 rpm, 4 °C). The supernatant was filtered through 0.2 µm PTFE filters (VWR, PA, USA) and subsequently analysed by reverse-phase high-performance liquid chromatography (HPLC) Dionex UltiMate 3000 LC system (ThermoFisher Scientific, MA, USA)[81]. Diagnostic pigments were converted to estimate contributions of different phytoplankton types using CHEMTAX [82], with initial pigment ratios according to [83]. Total chlorophyll-a derived from HPLC include both chlorophyll-a and divinyl chlorophyll-a, and is referred to as chlorophyll-a throughout this study.

Bacterial cell counts

Bacterial cells were stained with 1×SYBR Green I (Thermo Fisher Scientific, MA, USA) for 15 min and then quantified using a flow cytometer Accuri™ C6 (BD Biosciences, NJ, USA). Counts were processed using R package 'flowWorkspace' v4.18.0 [84] and stained cells were quantified using the 'gate_flowclust_2d' function in R package 'openCyto' [85].

353 **BEVs isolation and purification**
354 A sub-sample of 100 mL of concentrated seawater was further concentrated about 30 times to a final
355 volume of 3 mL using Vivaspin centrifugal filter units (Sartorius, Germany) with a 100 kDa cut-off.
356 The entire concentrate was then loaded onto an iodixanol density gradient following a published
357 protocol [86], and centrifuged at 100,000×g at 4°C for 6 hours. In the 15-30% and 35-40% fractions, the
358 iodixanol solution was exchanged twice with 1×PBS using Vivaspin centrifugal filter units with a 100
359 kDa cut-off at 2000×g, and resuspended in 1 mL 1×PBS. From each purified fraction, 800 µL was used
360 for molecular analyses and 200 µL for quantification of BEVs.

361 **Nanoparticle tracking analysis**
362 The abundance of BEVs was measured by nanoparticle tracking analysis (NTA) using a NanoSight
363 NS300 instrument (Malvern Panalytycal, UK) equipped with a 488 nm laser. Each sample was injected
364 using a syringe pump with a flow speed of 100 µL min^{-1}, and five videos of 60 sec were recorded.
365 Videos were analysed using NanoSight NTA software v3.2. All particles in the size up to 300 nm in
366 both the 15-30% and 35-40% fractions were included in the final abundance estimates. The flow cell
367 was thoroughly flushed with Milli-Q water (Merck Millipore) between samples, and visually examined
368 to exclude carry over. The performance of the instrument was routinely checked by measuring the
369 concentration and size distribution of standardized 100 nm silica beads.

370 **Metagenomics workflow**
371 One third of the polycarbonate filters with a pore size of 0.22 µm were used for the extraction of
372 genomic DNA using the DNeasy PowerWater Kit (QIAGEN N.V., Germany) according to the
373 manufacturer's recommendations. The extracted DNA was subject to enzymatic shearing and then
374 shotgun sequencing, performed on two lanes of the NovaSeq S4 platform (Illumina, Inc., CA, USA) at
375 the Vienna Biocenter Core Facilities (https://www.viennabiocenter.org/vbcf/ next-generation-
376 sequencing/).

377 The sequences from all samples were subject to the snakemake [87] metagenomic workflow in Anvi'o v8
378 [88], with recommended parameters. Briefly, the raw FASTQ files were subject to quality control by
379 'illumina-utils' v2.13 [89] and taxonomic classification using KrakenUniq v1.0.4 [90] and analysed using R
380 package 'pavian' v1.2.1 [91]. Then the reads were assembled using MEGAHIT v1.2.9 [92] and the gene
381 calling was performed using Prodigal v2.6.3 [93]. To construct the database for downstream
382 metaproteomic analysis, protein-coding genes were clustered at 99% similarity using CD-HIT v4.6.881
383 [94].

384 Taxonomic affiliation of the gene calls was estimated using Kaiju v1.9.2 [95] against the NCBI RefSeq
385 database (date: 2024-08-14), followed by classification of sequences with unknown taxonomic
386 affiliation against the NCBI nr database (date: 2024-08-25). Functional annotation of the genes was
387 carried out against InterPro v98 [96], NCBIfam v17.0 [97], Pfam v37 [98] databases using InterProScan v5.66
388 [99]. The unidentified protein sequences with no hits, were assigned taxonomy and function using
389 BLASTp [100] best-hit approach, against NCBI RefSeq database (date: 2025-01-27). Protein sub-cellular
390 localization was estimated using a combination of PSORTb v3.0.6 [101] and Phobius v1.01 [102].

391 **Proteomics workflow**
392 We used the remaining two thirds of the polycarbonate filters with a pore size of 0.22 µm for extraction
393 of cellular proteins. Protein extraction from the filter was performed as described in detail by [103].
394 Briefly, the filters were ground into small pieces with a sterile metal spatula after submerging the
395 tubes with the filters into liquid nitrogen. Filter pieces were resuspended in lysis buffer (100mM
396 Tris-HCl pH 7.4, 1% SDS, 150mM NaCl, 1mM DTT, 10mM EDTA) and cells were lysed with five
397 freeze-and-thaw cycles. After centrifugation (20,000x *g* at 4°C for 25 min) the supernatant was
398 transferred into a tube and proteins were co-precipitated with 0.015% deoxycholate and 7%
399 trichloroacetic acid (TCA) on ice for 1h and washed twice with ice-cold acetone. Dried protein
400 pellets were resuspended in 50 mM TEAB buffer (Millipore Sigma, Burlington, MA, USA) and
401 cysteines were reduced and alkylated with 10 mM DTT and 55 mM iodoacetamide (IAA),
402 respectively. To extract proteins associated with the BEVs, we added the sample reducing agent
403 NuPAGE (Invitrogen, Waltham, MA, USA) to 600 µL of purified BEVs at 1X final concentration.

All samples were re-precipitated using 9 times the sample volume of 96% EtOH at -20°C overnight. Pellets were resuspended in 50 mM TEAB, followed by overnight in-solution trypsin (Roche, Basel, Switzerland) digestion (1:100, w/w) at 37°C. TFA was added to the samples at 1% final concentration to terminate trypsin digestion. Samples were desalted using Pierce C18 Tips (ThermoFisher Scientific, MA, USA) according to the manufacturer's protocol. Prior the LC-MS analysis, digested peptides were dissolved in 0.1% formic acid and 2% acetonitrile.

Purified tryptic peptides were dissolved in 0.1% formic acid (FA) and measured using a nano-reversed-phase high-performance liquid chromatography (RP-HPLC) system Dionex Ultimate 3000 (ThermoFisher Scientific, MA, USA), coupled with a benchtop Quadrupole Orbitrap mass spectrometer Q-Exactive Plus (ThermoFisher Scientific, MA, USA). Peptides were separated on a PepMap RSLC C18 column (ThermoFisher Scientific, MA, USA) at 55°C with a flow rate of 300 nL/min. The two-hour segmented LC gradient ranged from 5% to 80% buffer B (79.9% acetonitrile, 0.1% FA). Mass spectra were acquired in positive ion mode using a top-15 data-dependent acquisition method. Full MS scans were performed at a resolution of 70,000 (*m/z* 200), followed by MS/MS scans at a resolution of 17,500. High-energy collisional dissociation (HCD) fragmentation was applied with a normalized collision energy (NCE) of 30%. Dynamic exclusion was set to 60 seconds.

The MS raw files of proteins extracted from the bacterial cells and the BEVs were searched using SEQUEST-HT against the bacterial protein coding genes from the co-assembled metagenome. Search parameters were as follows: enzyme - trypsin, fragment mass tolerance - 0.8 Da, max. missed cleavages - 2, fixed modifications - carbamidomethyl (Cys), optional modifications - oxidation (Met). Percolator parameters were as follows: max. delta Cn: 0.6, max. rank: 0, validation based on q-value, false discovery rate (calculated by automatic decoy searches) 0.05. Only proteins with more than two peptides and at least one unique peptide were included in the statistical analyses.

Statistical analyses

Statistical analyses were done in R v4.4.2 (R Core Team 2022) using RStudio v2024.09.1 (RStudio Team 2019). Protein enrichment analysis was performed using the R package 'DEqMS' v1.22.0 [104] on a log2-transformed and median-centred protein abundance matrix. In the enrichment test, only those proteins were included that were observed in at least two samples in each fraction. All figures were generated using the R package 'ggplot2' v3.5.1 [105].

Data availability

The metagenomic raw sequences have been deposited in the European Nucleotide Archive (ENA) at EMBL-EBI under Project accession number PRJEB88044. The mass spectrometry proteomics data have been deposited to the ProteomeXchange Consortium [106] via the PRIDE [107] partner repository with the dataset identifier PXD062682.

Scripts for data processing and statistical analyses, as well as raw flow cytometry and NTA files, can be accessed via Zenodo (https://www.zenodo.org/) under doi: 10.5281/zenodo.15772523 and 10.5281/zenodo.15772578, respectively.

Author contributions

EF performed fieldwork, the bioinformatic and statistical analyses, and wrote the manuscript. EF and GJH designed the project. EF, NO, TT performed the protein extraction and LAS carried out the LC-MS measurements. HL, ZY and TJB performed the phytoplankton pigment sampling and analyses. EPA was the chief scientist on board and coordinated the sampling. DS and SJB contributed to data interpretation. All authors contributed to the manuscript and approved its submitted version.

Acknowledgments

We thank the captain, the crew and the scientific team of the RV SONNE SO289 GEOTRACES research expedition ('S Pacific GEOTRACES', 03G0289NA, funded by the Bundesministerium für Bildung und Forschung (BMBF)). We thank A. Mutzberg, D. Jasinski, F. Evers, T. Schott, K.

Nachtigall and T. Klüver for technical support. We thank Z. Steiner for his support during the expedition. M. Aubert for assistance with laboratory sample processing. EF acknowledges funding by the Austrian Science Fund (FWF) M2797-B. This work was also supported by the Austrian Science Fund (FWF) project I4978-B to GJH and by the Slovenian Research Agency (ARIS) project J7-2599 to TT.

References

1. Kulp, A. & Kuehn, M. J. Biological functions and biogenesis of secreted bacterial outer membrane vesicles. *Annu. Rev. Microbiol.* **64**, 163–184 (2010).
2. Knox, K. W., Vesk, M. & Work, E. Relation between excreted lipopolysaccharide complexes and surface structures of a lysine-limited culture of Escherichia coli. *J. Bacteriol.* **92**, 1206–1217 (1966).
3. Toyofuku, M., Schild, S., Kaparakis-Liaskos, M. & Eberl, L. Composition and functions of bacterial membrane vesicles. *Nat. Rev. Microbiol.* (2023) doi:10.1038/s41579-023-00875-5.
4. Bitto, N. J. *et al.* Bacterial membrane vesicles transport their DNA cargo into host cells. *Sci. Rep.* **7**, 7072 (2017).
5. Tran, F. & Boedicker, J. Q. Genetic cargo and bacterial species set the rate of vesicle-mediated horizontal gene transfer. *Sci. Rep.* **7**, 8813 (2017).
6. Yaron, S., Kolling, G. L., Simon, L. & Matthews, K. R. Vesicle-mediated transfer of virulence genes from Escherichia coli O157:H7 to other enteric bacteria. *Appl. Environ. Microbiol.* **66**, 4414–4420 (2000).
7. Renelli, M., Matias, V., Lo, R. Y. & Beveridge, T. J. DNA-containing membrane vesicles of Pseudomonas aeruginosa PAO1 and their genetic transformation potential. *Microbiology* **150**, 2161–2169 (2004).
8. Johnston, E. L. *et al.* Planktonic and biofilm-derived Pseudomonas aeruginosa outer membrane vesicles facilitate horizontal gene transfer of Plasmid DNA. *Microbiol. Spectr.* e0517922 (2023).
9. Soler, N. & Forterre, P. Vesiduction: the fourth way of HGT. *Environ. Microbiol.* **22**, 2457–2460 (2020).
10. Toyofuku, M. *et al.* Membrane vesicle-mediated bacterial communication. *ISME J.* **11**, 1504–1509 (2017).

480 11. Mashburn, L. M. & Whiteley, M. Membrane vesicles traffic signals and facilitate group activities
481 in a prokaryote. *Nature* **437**, 422–425 (2005).
482 12. Yonezawa, H. *et al.* Outer membrane vesicles of Helicobacter pylori TK1402 are involved in
483 biofilm formation. *BMC Microbiol.* **9**, 197 (2009).
484 13. Li, Z., Clarke, A. J. & Beveridge, T. J. Gram-negative bacteria produce membrane vesicles which
485 are capable of killing other bacteria. *J. Bacteriol.* **180**, 5478–5483 (1998).
486 14. Kadurugamuwa, J. L. & Beveridge, T. J. Bacteriolytic effect of membrane vesicles from
487 Pseudomonas aeruginosa on other bacteria including pathogens: conceptually new antibiotics. *J.*
488 *Bacteriol.* **178**, 2767–2774 (1996).
489 15. Zlatkov, N., Nadeem, A., Uhlin, B. E. & Wai, S. N. Eco-evolutionary feedbacks mediated by
490 bacterial membrane vesicles. *FEMS Microbiol. Rev.* (2020) doi:10.1093/femsre/fuaa047.
491 16. Orench-Rivera, N. & Kuehn, M. J. Environmentally controlled bacterial vesicle-mediated export.
492 *Cell. Microbiol.* **18**, 1525–1536 (2016).
493 17. Toyofuku, M., Tashiro, Y., Hasegawa, Y., Kurosawa, M. & Nomura, N. Bacterial membrane
494 vesicles, an overlooked environmental colloid: Biology, environmental perspectives and
495 applications. *Adv. Colloid Interface Sci.* **226**, 65–77 (2015).
496 18. Bar-On, Y. M. & Milo, R. The Biomass Composition of the Oceans: A Blueprint of Our Blue
497 Planet. *Cell* **179**, 1451–1454 (2019).
498 19. Browning, T. J. *et al.* Nutrient co-limitation at the boundary of an oceanic gyre. *Nature* **551**, 242–
499 246 (2017).
500 20. Capone, D. G. & Hutchins, D. A. Microbial biogeochemistry of coastal upwelling regimes in a
501 changing ocean. *Nat. Geosci.* **6**, 711–717 (2013).
502 21. Moore, C. M. *et al.* Processes and patterns of oceanic nutrient limitation. *Nat. Geosci.* **6**, 701–710
503 (2013).
504 22. Zoccarato, L., Sher, D., Miki, T., Segrè, D. & Grossart, H.-P. A comparative whole-genome
505 approach identifies bacterial traits for marine microbial interactions. *Commun Biol* **5**, 276 (2022).
506 23. Stocker, R. Marine microbes see a sea of gradients. *Science* **338**, 628–633 (2012).

24. Worden, A. Z. *et al.* Environmental science. Rethinking the marine carbon cycle: factoring in the multifarious lifestyles of microbes. *Science* **347**, 1257594 (2015).

25. Kirchman, D. L. The uptake of inorganic nutrients by heterotrophic bacteria. *Microb. Ecol.* **28**, 255–271 (1994).

26. Reintjes, G., Arnosti, C., Fuchs, B. M. & Amann, R. An alternative polysaccharide uptake mechanism of marine bacteria. *ISME J.* **11**, 1640–1650 (2017).

27. Tortell, P. D., Maldonado, M. T., Granger, J. & Price, N. M. Marine bacteria and biogeochemical cycling of iron in the oceans. *FEMS Microbiol. Ecol.* **29**, 1–11 (1999).

28. Koch, A. L. What size should a bacterium be? A question of scale. *Annu. Rev. Microbiol.* **50**, 317–348 (1996).

29. Gasol, J. M., del Giorgio, P. A., Massana, R. & Duarte, C. M. Active versus inactive bacteria:size-dependence in a coastal marine plankton community. *Mar. Ecol. Prog. Ser.* **128**, 91–97 (1995).

30. Fischer, T. *et al.* Biopearling of Interconnected Outer Membrane Vesicle Chains by a Marine Flavobacterium. *Appl. Environ. Microbiol.* **85**, (2019).

31. Dürwald, A. *et al.* Reaching out in anticipation: bacterial membrane extensions represent a permanent investment in polysaccharide sensing and utilization. *Environ. Microbiol.* **23**, 3149–3163 (2021).

32. Fadeev, E. *et al.* Characterization of membrane vesicles in Alteromonas macleodii indicates potential roles in their copiotrophic lifestyle. *Microlife* **4**, 2022.09.27.509651 (2023).

33. Biller, S. J. *et al.* Bacterial vesicles in marine ecosystems. *Science* **343**, 183–186 (2014).

34. Biller, S. J. *et al.* Prochlorococcus extracellular vesicles: molecular composition and adsorption to diverse microbes. *Environ. Microbiol.* (2021) doi:10.1111/1462-2920.15834.

35. Biller, S. J. *et al.* Environmental and Taxonomic Drivers of Bacterial Extracellular Vesicle Production in Marine Ecosystems. *Appl. Environ. Microbiol.* e0059423 (2023).

36. Linney, M. D. *et al.* Microbial Sources of Exocellular DNA in the Ocean. *Appl. Environ. Microbiol.* **88**, e0209321 (2022).

37. Lücking, D., Mercier, C., Alarcón-Schumacher, T. & Erdmann, S. Extracellular vesicles are the main contributor to the non-viral protected extracellular sequence space. *ISME Commun* **3**, 112 (2023).

38. Liu, H. *et al.* Patterns of (micro)nutrient limitation across the South Pacific Ocean. *Commun. Earth Environ.* **5**, 1–9 (2024).

39. Teeling, H. *et al.* Recurring patterns in bacterioplankton dynamics during coastal spring algae blooms. *Elife* **5**, e11888 (2016).

40. Pontiller, B. *et al.* Rapid bacterioplankton transcription cascades regulate organic matter utilization during phytoplankton bloom progression in a coastal upwelling system. *ISME J.* **16**, 2360–2372 (2022).

41. Morris, R. M. *et al.* SAR11 clade dominates ocean surface bacterioplankton communities. *Nature* **420**, 806–810 (2002).

42. Reintjes, G. *et al.* On-site analysis of bacterial communities of the ultraoligotrophic South Pacific Gyre. *Appl. Environ. Microbiol.* **85**, (2019).

43. Oggerin, M. *et al.* Niche differentiation within bacterial key-taxa in stratified surface waters of the Southern Pacific Gyre. *ISME J.* **18**, (2024).

44. Zhang, Z. *et al.* Substantial trace metal input from the 2022 Hunga Tonga-Hunga Ha'apai eruption into the South Pacific. *Nat. Commun.* **15**, 8986 (2024).

45. Biller, S. J. *et al.* Membrane vesicles in sea water: heterogeneous DNA content and implications for viral abundance estimates. *ISME J.* **11**, 394–404 (2017).

46. Soler, N., Krupovic, M., Marguet, E. & Forterre, P. Membrane vesicles in natural environments: a major challenge in viral ecology. *The ISME journal* vol. 9 793–796 (2015).

47. Nekrouf, N. A., Maestre-Carballa, L., Lluesma-Gomez, M., Martinez-Hernandez, F. & Martínez-García, M. Annual dynamics and metagenomics of marine vesicles: One more layer of complexity in the dissolved organic fraction. *Limnol. Oceanogr.* (2025) doi:10.1002/lno.70031.

48. Schwechheimer, C., Sullivan, C. J. & Kuehn, M. J. Envelope control of outer membrane vesicle production in Gram-negative bacteria. *Biochemistry* **52**, 3031–3040 (2013).

560 49. Minhas, T. & Greenman, J. Production of cell-bound and vesicle-associated trypsin-like protease,
561 alkaline phosphatase and N-acetyl-beta-glucosaminidase by Bacteroides gingivalis strain W50. *J.*
562 *Gen. Microbiol.* **135**, 557–564 (1989).
563 50. Sabra, W., Lünsdorf, H. & Zeng, A.-P. Alterations in the formation of lipopolysaccharide and
564 membrane vesicles on the surface of Pseudomonas aeruginosa PAO1 under oxygen stress
565 conditions. *Microbiology* **149**, 2789–2795 (2003).
566 51. Gerritzen, M. J. H. *et al.* High dissolved oxygen tension triggers outer membrane vesicle formation
567 by Neisseria meningitidis. *Microb. Cell Fact.* **17**, 157 (2018).
568 52. Orench-Rivera, N. & Kuehn, M. J. Differential Packaging Into Outer Membrane Vesicles Upon
569 Oxidative Stress Reveals a General Mechanism for Cargo Selectivity. *Front. Microbiol.* **12**,
570 561863 (2021).
571 53. Pérez-Cruz, C., Delgado, L., López-Iglesias, C. & Mercade, E. Outer-inner membrane vesicles
572 naturally secreted by gram-negative pathogenic bacteria. *PLoS One* **10**, e0116896 (2015).
573 54. Morel, F. M. M. & Price, N. M. The biogeochemical cycles of trace metals in the oceans. *Science*
574 **300**, 944–947 (2003).
575 55. Prados-Rosales, R. *et al.* Role for Mycobacterium tuberculosis membrane vesicles in iron
576 acquisition. *J. Bacteriol.* **196**, 1250–1256 (2014).
577 56. Wang, M., Nie, Y. & Wu, X.-L. Membrane vesicles from a Dietzia bacterium containing multiple
578 cargoes and their roles in iron delivery. *Environ. Microbiol.* **23**, 1009–1019 (2021).
579 57. Lin, J. *et al.* A Pseudomonas T6SS effector recruits PQS-containing outer membrane vesicles for
580 iron acquisition. *Nat. Commun.* **8**, 14888 (2017).
581 58. Dhurve, G., Madikonda, A. K., Jagannadham, M. V. & Siddavattam, D. Outer Membrane Vesicles
582 of Acinetobacter baumannii DS002 Are Selectively Enriched with TonB-Dependent Transporters
583 and Play a Key Role in Iron Acquisition. *Microbiol Spectr* **10**, e0029322 (2022).
584 59. Hopkinson, B. M. & Barbeau, K. A. Iron transporters in marine prokaryotic genomes and
585 metagenomes. *Environ. Microbiol.* **14**, 114–128 (2012).
586 60. Armstrong, E., Granger, J., Mann, E. L. & Price, N. M. Outer-membrane siderophore receptors of
587 heterotrophic oceanic bacteria. *Limnol. Oceanogr.* **49**, 579–587 (2004).

588 61. Hogle, S. L. *et al.* Siderophores as an iron source for picocyanobacteria in deep chlorophyll
589 maximum layers of the oligotrophic ocean. *ISME J.* **16**, 1636–1646 (2022).
590 62. Noinaj, N., Guillier, M., Barnard, T. J. & Buchanan, S. K. TonB-dependent transporters:
591 regulation, structure, and function. *Annu. Rev. Microbiol.* **64**, 43–60 (2010).
592 63. Frias, A., Manresa, A., de Oliveira, E., López-Iglesias, C. & Mercade, E. Membrane vesicles: a
593 common feature in the extracellular matter of cold-adapted antarctic bacteria. *Microb. Ecol.* **59**,
594 476–486 (2010).
595 64. Wietz, M., López-Pérez, M., Sher, D., Biller, S. J. & Rodriguez-Valera, F. Microbe Profile:
596 Alteromonas macleodii - a widespread, fast-responding, "interactive" marine bacterium.
597 *Microbiology* **168**, (2022).
598 65. Manck, L. E. *et al.* Petrobactin, a siderophore produced by Alteromonas, mediates community iron
599 acquisition in the global ocean. *ISME J.* **16**, 358–369 (2022).
600 66. Manck, L. E., Espinoza, J. L., Dupont, C. L. & Barbeau, K. A. Transcriptomic Study of Substrate-
601 Specific Transport Mechanisms for Iron and Carbon in the Marine Copiotroph Alteromonas
602 macleodii. *mSystems* **5**, (2020).
603 67. Qiu, G.-W. *et al.* A unique porin meditates iron-selective transport through cyanobacterial outer
604 membranes. *Environ. Microbiol.* **23**, 376–390 (2021).
605 68. Qiu, G.-W., Koedooder, C., Qiu, B.-S., Shaked, Y. & Keren, N. Iron transport in cyanobacteria -
606 from molecules to communities. *Trends Microbiol.* **30**, 229–240 (2022).
607 69. Grossart, H.-P., Kiørboe, T., Tang, K. & Ploug, H. Bacterial colonization of particles: growth and
608 interactions. *Appl. Environ. Microbiol.* **69**, 3500–3509 (2003).
609 70. Seymour, J. R., Amin, S. A., Raina, J.-B. & Stocker, R. Zooming in on the phycosphere: the
610 ecological interface for phytoplankton–bacteria relationships. *Nature Microbiology* **2**, 1–12
611 (2017).
612 71. Kashtan, N. *et al.* Single-cell genomics reveals hundreds of coexisting subpopulations in wild
613 Prochlorococcus. *Science* **344**, 416–420 (2014).

614 72. Pham, A. L.-D., Aumont, O., Ratnarajah, L. & Tagliabue, A. Examining the interaction between
615 free-living bacteria and iron in the global ocean. *Global Biogeochem. Cycles* **36**, e2021GB007194
616 (2022).
617 73. Knoke, L. R. *et al.* Agrobacterium tumefaciens Small Lipoprotein Atu8019 Is Involved in
618 Selective Outer Membrane Vesicle (OMV) Docking to Bacterial Cells. *Front. Microbiol.* **11**, 1228
619 (2020).
620 74. Unfried, F. *et al.* Adaptive mechanisms that provide competitive advantages to marine
621 bacteroidetes during microalgal blooms. *ISME J.* **12**, 2894–2906 (2018).
622 75. Kappelmann, L. *et al.* Polysaccharide utilization loci of North Sea Flavobacteriia as basis for using
623 SusC/D-protein expression for predicting major phytoplankton glycans. *ISME J.* **13**, 76–91 (2019).
624 76. Glenwright, A. J. *et al.* Structural basis for nutrient acquisition by dominant members of the human
625 gut microbiota. *Nature* **541**, 407–411 (2017).
626 77. Sartorio, M. G., Pardue, E. J., Scott, N. E. & Feldman, M. F. Human gut bacteria tailor extracellular
627 vesicle cargo for the breakdown of diet- and host-derived glycans. *Proc. Natl. Acad. Sci. U. S. A.*
628 **120**, e2306314120 (2023).
629 78. Naval, P. & Chandra, T. S. Characterization of membrane vesicles secreted by seaweed associated
630 bacterium Alteromonas macleodii KS62. *Biochem. Biophys. Res. Commun.* **514**, 422–427 (2019).
631 79. Li, J., Azam, F. & Zhang, S. Outer membrane vesicles containing signalling molecules and active
632 hydrolytic enzymes released by a coral pathogen Vibrio shilonii AK1. *Environ. Microbiol.* **18**,
633 3850–3866 (2016).
634 80. Arnosti, C. *et al.* The Biogeochemistry of Marine Polysaccharides: Sources, Inventories, and
635 Bacterial Drivers of the Carbohydrate Cycle. *Ann. Rev. Mar. Sci.* **13**, 81–108 (2021).
636 81. Van Heukelem, L. & Thomas, C. S. Computer-assisted high-performance liquid chromatography
637 method development with applications to the isolation and analysis of phytoplankton pigments. *J.*
638 *Chromatogr. A* **910**, 31–49 (2001).
639 82. Mackey, M. D., Mackey, D. J., Higgins, H. W. & Wright, S. W. CHEMTAX - a program for
640 estimating class abundances from chemical markers:application to HPLC measurements of
641 phytoplankton. *Mar. Ecol. Prog. Ser.* **144**, 265–283 (1996).

642 83. DiTullio, G. R. *et al.* Phytoplankton assemblage structure and primary productivity along 170°W
643 in the South Pacific Ocean. *Mar. Ecol. Prog. Ser.* **255**, 55–80 (2003).
644 84. Finak, G. & Jiang, M. *FlowWorkspace: Infrastructure for Representing and Interacting with Gated*
645 *and Ungated Cytometry Data Sets*. (2022).
646 85. Finak, G. *et al.* OpenCyto: an open source infrastructure for scalable, robust, reproducible, and
647 automated, end-to-end flow cytometry data analysis. *PLoS Comput. Biol.* **10**, e1003806 (2014).
648 86. Biller, S. J. *et al.* Isolation and Characterization of Cyanobacterial Extracellular Vesicles. *J. Vis.*
649 *Exp.* (2022) doi:10.3791/63481.
650 87. Köster, J. & Rahmann, S. Snakemake--a scalable bioinformatics workflow engine. *Bioinformatics*
651 **28**, 2520–2522 (2012).
652 88. Eren, A. M. *et al.* Community-led, integrated, reproducible multi-omics with anvi'o. *Nat.*
653 *Microbiol.* **6**, 3–6 (2021).
654 89. Eren, A. M., Vineis, J. H., Morrison, H. G. & Sogin, M. L. A filtering method to generate high
655 quality short reads using illumina paired-end technology. *PLoS One* **8**, e66643 (2013).
656 90. Breitwieser, F. P., Baker, D. N. & Salzberg, S. L. KrakenUniq: confident and fast metagenomics
657 classification using unique k-mer counts. *Genome Biol.* **19**, 198 (2018).
658 91. Breitwieser, F. P. & Salzberg, S. L. Pavian: interactive analysis of metagenomics data for
659 microbiome studies and pathogen identification. *Bioinformatics* **36**, 1303–1304 (2020).
660 92. Li, D., Liu, C.-M., Luo, R., Sadakane, K. & Lam, T.-W. MEGAHIT: an ultra-fast single-node
661 solution for large and complex metagenomics assembly via succinct de Bruijn graph.
662 *Bioinformatics* **31**, 1674–1676 (2015).
663 93. Hyatt, D. *et al.* Prodigal: prokaryotic gene recognition and translation initiation site identification.
664 *BMC Bioinformatics* **11**, 119 (2010).
665 94. Li, W. & Godzik, A. Cd-hit: a fast program for clustering and comparing large sets of protein or
666 nucleotide sequences. *Bioinformatics* **22**, 1658–1659 (2006).
667 95. Menzel, P., Ng, K. L. & Krogh, A. Fast and sensitive taxonomic classification for metagenomics
668 with Kaiju. *Nat. Commun.* **7**, 11257 (2016).

669 96. Blum, M. *et al.* InterPro: the protein sequence classification resource in 2025. *Nucleic Acids Res.*
670 **53**, D444–D456 (2025).
671 97. Li, W. *et al.* RefSeq: expanding the Prokaryotic Genome Annotation Pipeline reach with protein
672 family model curation. *Nucleic Acids Res.* **49**, D1020–D1028 (2021).
673 98. Mistry, J. *et al.* Pfam: The protein families database in 2021. *Nucleic Acids Res.* **49**, D412–D419
674 (2021).
675 99. Jones, P. *et al.* InterProScan 5: genome-scale protein function classification. *Bioinformatics* **30**,
676 1236–1240 (2014).
677 100. Camacho, C. *et al.* BLAST+: architecture and applications. *BMC Bioinformatics* **10**, 421 (2009).
678 101. Lau, W. Y. V. *et al.* PSORTdb 4.0: expanded and redesigned bacterial and archaeal protein
679 subcellular localization database incorporating new secondary localizations. *Nucleic Acids Res.*
680 **49**, D803–D808 (2021).
681 102. Flores-Uribe, J. Identification of proteins containing transmembrane domains using Phobius v1.
682 (2018) doi:10.17504/protocols.io.pdwdi7e.
683 103. Tinta, T. *et al.* Microbial Processing of Jellyfish Detritus in the Ocean. *Front. Microbiol.* **11**,
684 590995 (2020).
685 104. Zhu, Y. *DEqMS*. (Bioconductor, 2018). doi:10.18129/B9.BIOC.DEQMS.
686 105. Villanueva, R. A. M. & Chen, Z. J. ggplot2: Elegant Graphics for Data Analysis (2nd ed.).
687 *Measurement (Mahwah NJ)* **17**, 160–167 (2019).
688 106. Deutsch, E. W. *et al.* The ProteomeXchange consortium at 10 years: 2023 update. *Nucleic Acids*
689 *Res.* **51**, D1539–D1548 (2023).
690 107. Perez-Riverol, Y. *et al.* The PRIDE database resources in 2022: a hub for mass spectrometry-based
691 proteomics evidences. *Nucleic Acids Res.* **50**, D543–D552 (2022).